Structural behavior of recycled aggregates concrete filled steel tubular columns

Boshra Eltaly *, Ahmed Bembawy, Nageh N. Meleka, Kameel Kandil

Department of Civil Engineering, Menoufia University, Shebin ElKoum, Menofia, Egypt

ABSTRACT

This paper presents an experimental and numerical investigation to determine the behavior of steel tubular columns filled with recycled aggregates concrete up to failure under constant axial compression loads. The experimental program included two steel tube columns, four recycled concrete columns and eight composite columns filled with different types of recycled coarse aggregates (granite and ceramic). Different percentages of recycled coarse aggregates: 0, 25 and 50 of the percentage of the coarse aggregates (dolomite) were used. The results of the numerical model that was employed by the finite element program, ANSYS, were compared with the experimental results. The results of the experimental study and the finite element analysis were compared with the design equations using different national building codes: AISC1999, AISC2005 and EC4. The results indicated that the recycled aggregates concrete infill columns have slightly lower but comparable ultimate capacities compared with the specimens filled with normal concrete.

ARTICLE INFO

1. Introduction

Composite section is defined as a structural element composed of two or more different materials. These materials are joined together to act as one unit. There are several types of composite elements in civil structures; composite column, beam and slab. Many kinds of composite column have been widely used included steel-concrete (the steel may be wide-flange, box, I or any shape), steel-wood, wood-concrete, and plastic-concrete or advanced composite materials-concrete. Hollow structural (square or rectangular) steel sections are often filled with concrete to form a composite column. Such kinds of composite columns have been the interest of structural engineers because of their high load bearing capacity. In these columns, steel box (rectangular or square) plates can only buckle outward locally under compression due to the restraints of the concrete core. This buckling mode leads to a considerable increase in the critical local buckling strength of the steel box. Also the ductility of concrete core is remarkably improved because of the steel box completely encases the concrete core. Additionally using these kinds of composite columns saves the materials and speeds the construction processes because of working the steel plates as longitudinal reinforcements and permanent formworks for the concrete core (Schneider, 1998; Uy, 1998; Shanmugam and Lakshmi, 2001; Uy, 2001; Bradford et al., 2002; Sakino et al., 2004; Lam and Gardner, 2008; Chen and Jin, 2010; Liang, 2012).

Recycled Aggregates Concrete (RAC) can be recognized as a new kind of concrete construction, in which, broken pieces of waste stone, ceramic, brick or concrete are used as coarse aggregates. The physical properties of RAC depend on both adhered mortar quality and the amount of adhered mortar. The previous published researches in the field of RAC concluded that it has low strength and elastic modulus, bad workability, high water infiltration and high shrinkage and creep so that they should be only used as nonstructural concrete. Also these results indicated that recycled aggregates concrete showed similar shear crack distributions as the natural aggregates concrete. Also they indicated that natural aggregates concrete specimens had bond strengths that

were 9 to 19% higher than the equivalent RAC specimens. However, RAC is well recognized in view of its low thermal conductivity, low brittleness as well as the low specific gravity that reduces the self-weight of the structures. Most importantly, the use of RAC can save natural resources and protect our living environment (Gomez-Soberon, 2002;Poon et al., 2004; Oikonomou, 2005; Etxeberria et al., 2007; Marco Breccolotti and Materazzi, 2010; Butler et al., 2011; Schubert et al., 2012; Campian et al., 2015). Evangelista and de Brito (2007) and Zega and Di Maio (2011) made concretes with recycled fine aggregates (RFA) replacing different percentages of natural river sand. Their results indicated that the compressive strengths of concretes made with 20% and 30% of recycled fine aggregates are similar to those of concrete made with 100% of natural fine aggregates.

A total of fourteen specimens were cast and tested to determine the behavior of Recycled Aggregates Concrete Filled Steel Tube Columns (RACFSTC) under axial loads up to failure. Different percentages of recycled coarse aggregates; 0, 25 and 50% of the natural coarse aggregates (dolomite) were used. The effect of composite action and the steel tube shape were studied. Their behavior includes the mode of failure, the ultimate capacity and the longitudinal strain. Also the buckling of the specimens was examined. The composite specimens were simulated by the FE program, ANSYS and their results were compared with the experimental test results. Additionally the results of the experimental study and the finite element analysis were compared with the design equations using different national building codes such as the AISC1999, AISC2005 and EC4.

2. Experimental Program

The experimental program considered four sets of test specimens giving a total of fourteen circular and square cross section columns as presented in Table 1. The specimens are with 1200 mm length, 100 mm diameter for the circular cross section specimens, 100 mm width for the box columns and 2 mm thickness as shown in Fig. 1. Their length-to-their depth and their depth-to-their tube thickness ratios remained a constant of 12 and 50; respectively. The first set of tests (S1) was designed to load the steel only and it included the control specimens; C&S specimens. The second set of tests (S2) consisted of four specimens: PC-C, R25G-C, R25C-C and R25G-C specimen and they was designed to load the concrete only and they are with circular cross section. The third set of tests (S3) was designed to load the composite section uniformly. They included four specimens; (CPC-C, CR25G-C, CR25C-C and CR25G-C). Four box columns; CPC-S, CR25G-S, CR25C-S and CR25G-S were categorized as set four (S4). In set two, set three and set four of the tests, four different types of concrete were used; plain concrete (PC100%), concrete with Recycled (R) Ceramics (C) and Granite (G) as a coarse aggregates replaced the natural coarse aggregates in plain concrete by percentage of 25% and 50% (RAC 25%G, RAC 25%C and RAC 50%G).

Table 1. Specimen details.

| No. Set	Specimen Code	Specimens Designation	Concrete Code	Steel Thickness	D/t	L/D
S1	C	Circle	Empty Section	2 mm	5	12
	S	Square			5	5
S2	PC-C	Circle	PC100%	No Steel	5	12
	R25G-C		RAC25%G		5	12
	R25C-C		RAC25%C		5	12
	R50G-C		RAC50%G		5	12
S3	CPC-C	Circle	PC100%	2mm	5	12
	CR25G-C		RAC25% G		5	12
	CR25C-C		RAC25% C		5	12
	CR50G-C		RAC50% G		5	12
S4	CPC-S	Square	PC100%	2mm	5	12
	CR25G-S		RAC25% G		5	12
	CR25C-S		RAC25% C		5	12
	CR25C-S		RAC25% C		5	12
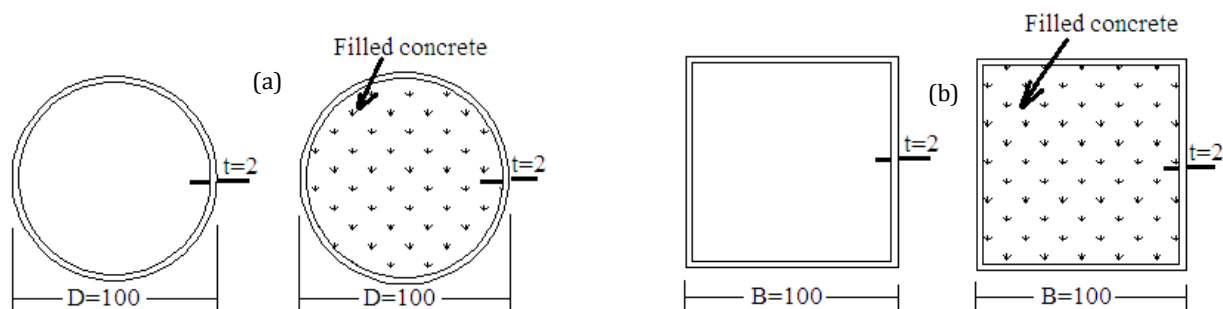
Fig. 1. Cross section details for hollow steel tube and concrete filled steel tube columns:
(a) Circular tube column; (b) Box column (all dimension in mm).

2.1. Constituent materials

The cement used was Egyptian Ordinary Portland Cement (E.S.S. 4756-1/2009). The density of the cement was 3.16 g/cm³ and the specific surface was 3.5 cm²/g. The chemical composition of the cement is shown in Table 2. Local sand from natural sources, clean and free from deleterious substances was used. The used coarse aggregates was commercially available (dolomite) and two RCA with different replacement percentages of the natural coarse aggregates were used; recycled ceramics and granite (Fig. 2). The physical properties of the aggregates are illustrated in Table 3. Sieve analyses were conducted for the fine and the coarse aggregates used and their results were performed and compared with the limits of the Egyptian Standard Specifications (E.S.S. 1109/2008), as shown in Tables 4 and 5; respectively. Clear water free from impurities was used for mixing. No chemical and mineral admixture was used in this study. The steel tubes are made from steel with properties indicated in Table 6.

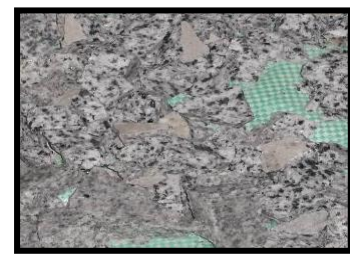**Table 2.** Chemical compositions of cement (%).

AL_2O_3	SiO_2	Fe_2O_3	CaO	MgO	SO3	k_2O	L.C.F
5.6	19.8	2.4	65.9	2.54	2.8	0.58	98.9

(a) Dolomite   (b) Recycled ceramics   (c) Recycled granite

Fig. 2. Natural and recycled coarse aggregates.

Table 3. Physical properties of the aggregates used.

Properties	Sand	Coarse Aggregates		
		Natural	Recycled	
			Ceramic	Granite
Mass (g/m³)	1.73	1.75	1.55	1.7
Specific Gravity (g/cm³)	2.6	2.7	2.6	2.7
Water Absorption (%)				1.12

Table 4. Sieve analysis of sand used.

Sieve Size (mm)	0.15	0.35	0.7	1.4	2.83	4.75
% Passing by Weight	4	15	62	79	95	100
Limits of (E.E.S.)	10-0	30-10	80-60	100-75	100-85	100

Table 5. Sieve analysis of natural and recycled coarse aggregates.

	Sieve Size (mm)		2.36	4.75	9.5	12.5	20
	% Limits of (E.S.S.)		5-0	15-0	70-40	100-90	100
% Passing by Weight	Natural	Dolomite	2	9	59	100	100
	Recycled	Ceramic	3	12	60	100	100
		Granite	4	14	55	100	100

Table 6. Mechanical properties of steel.

Modulus of Elasticity (GPa)	Yielding Strength (MPa)	Tensile Strength (MPa)
200	235	350

2.2. Concrete mix design

The mortar mix was designed according to Egyptian code of practice (E.C.P. 203/2007). Table 6 shows one meter cube (m³) of the mixes. Twelve 150 x 150 x 150 mm cubes were cast and tested after 7 and 28 days, to determine the compressive strength of the matrix with the selected mortar mix. Compression test was carried out according to the E.S.S. (E.S.S. 2070/2007) on a hydraulic compression testing machine and the average strengths of the cubes are presented in Table 7. Also four 50 x 50 mm cylinders were cast and test to determine the splitting tensile stress of the mix after 28 days.

Table 7. Concrete mix and average strength for the plain concrete and recycled concrete.

Mix No.	Concrete Code	Concrete Mix (kg/m³)					Average Strength (MPa)		
							Compression		Tension
		C	W/C %	S	NCA	RCA	7 days	28 days	
1	PC 100%	450	0.55	920	752	0	25.8	36.26	3.82
2	RAC 25%G	450	0.55	935	532	220	24	33.48	3.38
3	RAC 25%C	450	0.55	915	564	188	22.5	32.0	3.25
4	RAC 50%G	450	0.55	935	376	376	22.5	32.4	3.2

2.3. Specimens preparation

The filled concrete specimen's preparation passed through three stages. At the first stage, the steel sections were prepared. Segments with 314 mm cutting width for box columns and with 400 mm for the specimens of the square sections and 1200 mm interrupted length were cutting from steel sheet 2000 x 1200 x 2 mm total dimensions. Then each piece was formed to be with required cross section and was welded using automatic submerged welding machine. Finally, sections were settled after removing welding impurities and were painted by insulator paint to prevent corrosion of steel during treatment. At the second stage, the top and the bottom base plate were prepared as shown in Fig. 3. At the third stage, the concrete was mixed and cast in the steel section (Fig. 4). Then the column was compacted during casting. Finally, the samples were treated in the water sector until two days before the test.
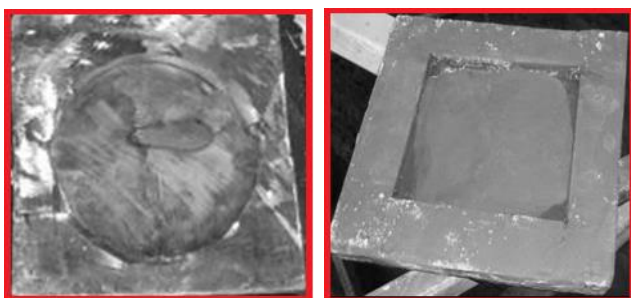
Fig. 3. Circular and box base plates.

Fig. 4. Mixing and casting concrete.

2.4. Test setup

The prepared specimen was inserted into a 5000 kN testing machine as shown in Fig. 5. Two base plates (30 mm thickness) were placed on the top and bottom ends of the specimens to ensure uniform load distribution. The loading rate was 50 kN per minute. A 2000 kN load cell was attached to the upper machine head to measure the load during testing. Two transducer springs LVDT's of length 50 mm was used to measure the lateral displacement of the tested columns as shown in Fig. 6. Two strain gauges were fixed longitudinally on the outside surface of the steel tubes to monitor the axial strain of the steel tube as illustrated in Fig. 6. All the instrumentations were connected to a data accusation system to record different measurements with a rate of recording of one reading per second.
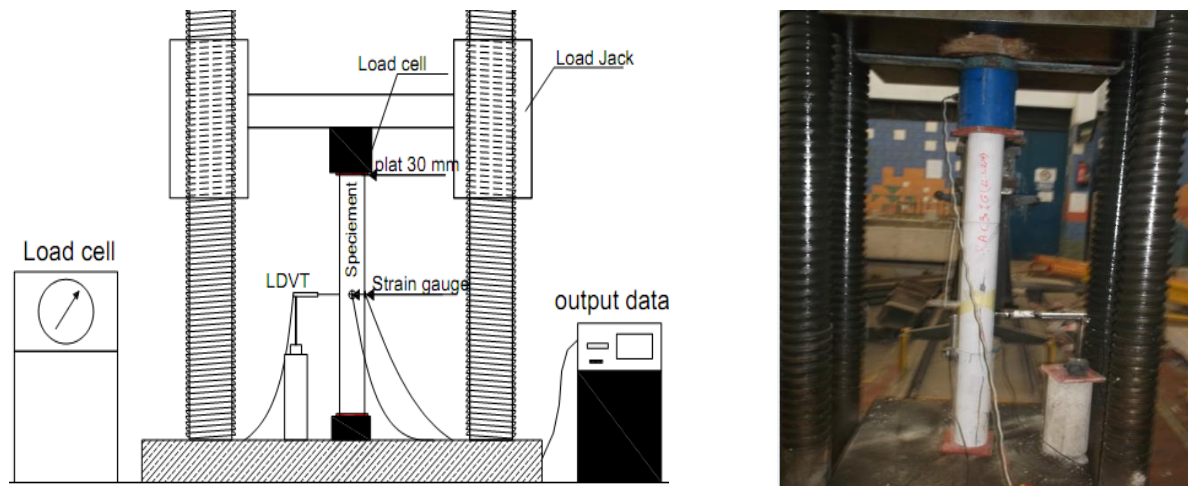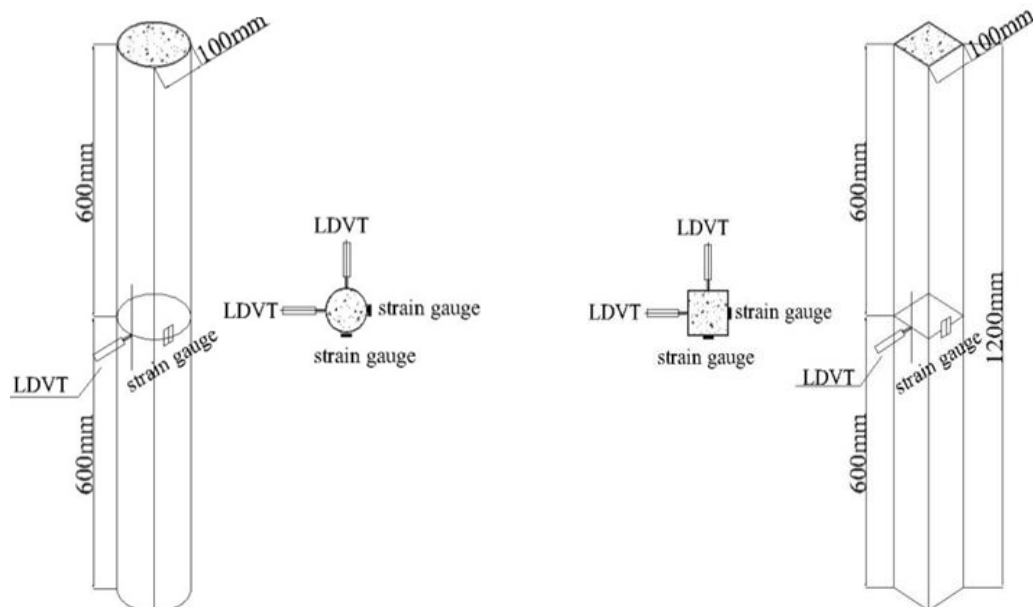
Fig. 5. Test machine and setup.

Fig. 6. Location of strain gauges and LVDTs.

3. Numerical Analysis

The composite tested columns were simulated by FE program; ANSYS 12. The current simulation model takes in consideration the geometry and the material nonlinearities. In this simulation, Soild65 elements were used for presented concrete (Fig. 7). Each element is defined by eight nodes and each node has three degrees of freedom (translations in the nodal x, y, and z directions). This element has cracking and crushing capabilities (ANSYS, 2006; Hoque, 2006; Singh, 2006; Aboul-Anen et al., 2009; Shaheen et al., 2013; Shaheen et al., 2014). Shell181 elements were used for modeling steel tube. Each element was defined by four or three nodes with six degree of freedoms at each node: translation in the x, y, and z directions and rotation about the x, y, and z directions as shown in Fig. 8. Shell181 element is well-suited for large rotation and large strain nonlinear applications (ANSYS, 2006; Patel and Lande, 2016). At the bottom of the column, all nodes had transition restraints in the x, y, and z directions.

At the top of the column, perimeter nodes were restrained in x, y, and z directions. All other nodes were free to translate or rotate at any direction. The FE model is illustrated in Fig. 9.
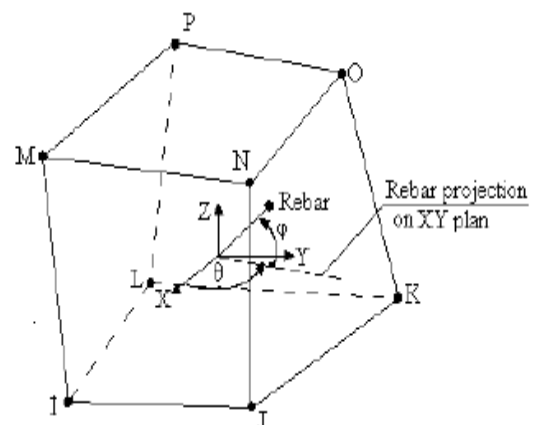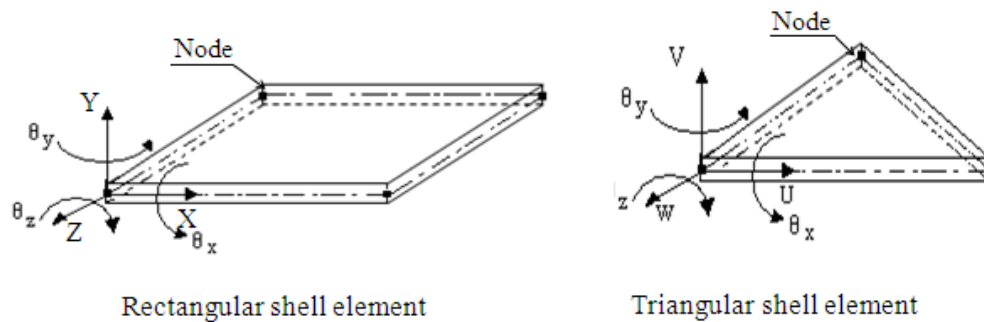

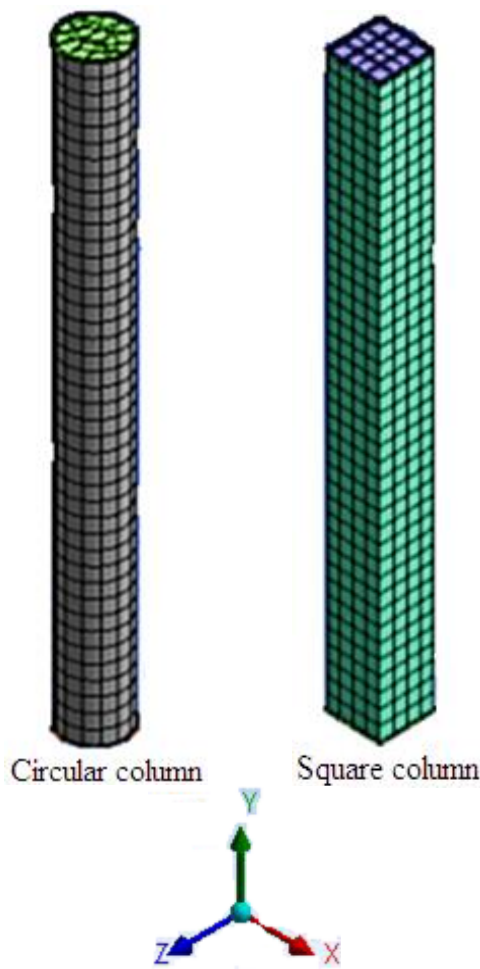**Fig. 7.** Solid65 element.

Fig. 8. Shell181 element.

Fig. 9. FE simulation.

to the program. The modulus of elasticity of concrete and stress-strain curve were calculated according to the Egyptian Code (E.C.P. 203/2007). By considering the compressive strength of concrete after 28 days (F_{cu} in MPa), The modulus of elasticity of concrete (E_c in MPa) can be calculated from Eq. (1). The multi-linear isotropic stress-strain curve for the concrete can be computed by Eq. (2). The stress-strain curve for the unconfined concrete mix is presented in Fig. 10.

$$E_c = 4400\sqrt{F_{cu}} \tag{1}$$

$$Stress = \frac{E_c \varepsilon}{1 + (\varepsilon/\varepsilon_0)^2} \tag{2}$$

$$\varepsilon_0 = \frac{2F_{cu}}{E_c} \tag{3}$$

(a)

Cracking is permitted in three orthogonal directions at each integration point and the cracking is modeled in ANSYS program. If cracking occurs at an integration point, the cracking is modeled through an adjustment of material properties which effectively treats the cracking as a smeared band of cracks, rather than discrete cracks (Wilson et al., 1973). Also if a crack is detected at an integration point, the stress-strain relationship is modified by introducing a plane of weakness in the direction normal to the crack face. To simulate the nonlinear behavior of the specimens, the modules of elasticity, the compressive and tensile strength of concrete after 28 days and the stress-strain curve of concrete mix must be defined
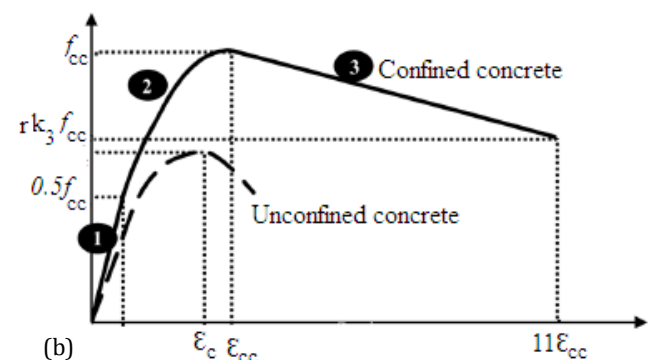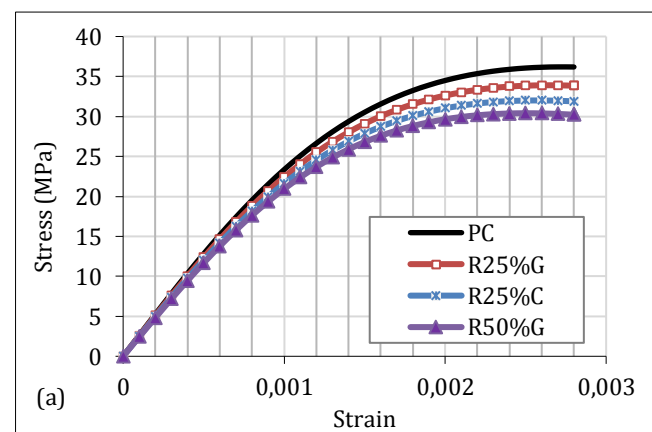

(b)

Fig. 10. Stress- strain curves for concrete used: (a) Unconfined concrete; (b) Confined concrete (Saenz, 1964).

The confinement provided by the steel tube on the concrete increases the strength and ductility of the concrete. This confinement depends on the steel depth-to-thickness (D/t) ratios. A lower value of D/t ratio gives high considerable confinement for the concrete however a higher D/t ratio provides failure of the columns due to local buckling of the steel tube (Mander et al., 1988; Zuboski, 2013). The compressive strength; f_{cc} of confined concrete and the corresponding confined strain; ε_{cc} were calculated from Eqs. (5) and (6); respectively (Mander et al., 1988). Where σ_{lat} is the lateral confining pressure imposed on the concrete by the steel tube and the factors k1 and k2 were considered as 4.1 and 20.5; respectively (Patton and Singh, 2014). The stress-strain curve of confined concrete is presented in Fig. 10. The first part of the curve is the elastic part up to the proportional limit ($0.5f_{cc}$). The second part of the curve starts from the proportional limit stress ($0.5f_{cc}$) to the f_{cc}. This part was adapted from Eqs. (7-9) (Patton and Singh, 2014). R_σ is the ratio of maximum compressive strength of concrete to the stress corresponding to maximum strain on stress-strain curve. R_ε is the ratio of maximum strain on stress-strain curve to the strain corresponding to maximum compressive strength. The two factors were considered as 4.0. The third part of the curve is used to describe the softening behavior of the concrete. It starts from f_{cc} to a value lower than or equal to rk_3f_{cc} and this part does not considered in the analysis.

$$f_{cc} = f_c + k_1 \sigma_{lat} \tag{4}$$

$$\varepsilon_{cc} = \varepsilon_c \left(1 + k_2 \frac{\sigma_{lat}}{f_c}\right) \tag{5}$$

$$f = \frac{E_{cc}\varepsilon}{1 + (R + R_E - 2)\left(\frac{\varepsilon}{\varepsilon_{cc}}\right) - (2R - 1)\left(\frac{\varepsilon}{\varepsilon_{cc}}\right)^2 + R\left(\frac{\varepsilon}{\varepsilon_{cc}}\right)^3} \tag{6}$$

$$R_E = \frac{E_{cc}\, \varepsilon_{cc}}{f_{cc}} \tag{7}$$

$$R = \frac{R_E(R_\sigma - 1)}{(R_\varepsilon - 1)^2} - \frac{1}{R_\varepsilon} \tag{8}$$

The behavior of the steel tube is modeled according to the simple plastic theory (Salem, 1970; Vazirani and Ratwani, 1996). According to their theory strain hardening is neglected. The relation between the stress and strain extends from zero stress and strain passing through the linear zone to the yield (σ_y) point and finally through zero slops horizontal part of the curve. To describe this relationship into the program, the steel sheet modulus of elasticity, yield stress and tangent modulus or strain hardening modulus were defined to the program as explained in the experimental work. In the current analysis, the load-control technique was considered. In this technique, the load was applied to the model and it was divided into a series of increments called load steps. The load steps were defined by program user. After completing each increment, the stiffness matrix of the model is adjusted to reflect nonlinear changes in structural stiffness. This change occurs before proceeding to the next load increment.

The ANSYS program uses Newton-Raphson method for updating the model stiffness. The design of composite columns is addressed by a large number of design specifications. AISC-LRFD (1999), AISC-LRFD (2005) and EC4 (2004) codes were used to determine the ultimate load of composite specimens and their results were compared with the numerical and experimental results.

4. Results and Discussion

The experimental results of the ultimate failure loads for all specimens tested are presented in Table 8. Fig. 11 showed the full collapse of all specimens tested as obtained from the experimental program. The effectives of the recycled concrete in the behavior of the long columns are presented in Figs. 12 and 13. Fig. 12 shows the load-strain curves for the four circular concrete columns and Fig. 13 represents the comparison between the ultimate loads for these columns.

Figs. 14 and 15 illustrate the experimental load-strain curves and load-lateral displacement curve for S3 specimens. Fig. 11 and Table 8 illustrate that the failure occurs in steel column due to local buckling and it occurs due to concrete crushing in the concrete columns. On the other hand the failure occurs in composite columns because of global buckling in specimens with circular cross sections and local buckling in all specimens with square cross sections except that CR50G-S specimen.

From Fig. 12, it can be seen that the load-strain curves for all the four specimens of S2 group are linear till the ultimate load then the load are decreased. Also Figs. 12 and 13 and Table 8 indicate that RAC columns have slightly lower comparable ultimate capacities compared with the normal concrete specimen. The ultimate capacities of the in filled steel circular column with normal concrete were about 16 and 8 percent higher than those containing 25 and 50 percent recycled granite coarse aggregates; respectively as shown in Figs. 14 and 15 and Table 8. Also these figures indicated that the specimen with The RAC 25C% concrete mix nearly achieved the same properties as the plain concrete mix maintaining the mix proportions and its production order the same.

The effect of composite action is presented in Fig. 16. From this figure, it can be seen that the ultimate loads of composite columns are 250 percent higher than concrete or steel columns. The strain at the mid-height for specimens with square cross section are measured and given in Figs. 17-19. These Figures show that the increasing ranges of ultimate load of plain concrete column are about 11 and 17 percent. Table 8 indicates that the ultimate strength in circular section column is 30 to 40 percent higher compared to square section. This is because circular section takes confining effect better than square section.

The deformed shapes of the test columns as observed from the tests were compared with the deformed shapes obtained from the finite element analysis. It was found that good agreement exists between the experimental and numerical deformed shapes of the columns as shown in Fig. 20. The experimental and numerical ultimate load-axial strain relationships for specimen

CR50G-C as a sample are presented in Fig. 21. The comparison between the ultimate loads of composite columns as obtained from the FE simulation and four design procedures are illustrated in Tables 9 and 10 for specimens with circular and square sections; respectively.

Results in Table 9 and Table 10 show that AISC-LRFD (1999), AISC-LRFD (2005) and EC4 (2004) are conservative for predicting the member capacities of the specimens with different RAC contents. Overall, AISC-LRFD (1999) and AISC-LRFD (2005) gives ultimate capacity about 11% and 7% respectively; lower than the results obtained from the tests. However, EC4 (2004) gives capacity of the column as presented in Table 8 and Table 9 about 2% higher than those of the measured ultimate strength, and from that it can be concluded that it is an unsafe predictor. Also the two tables show that the FE simulation gives acceptable results compared to the experimental results.

Table 8. Specimens' results.

No. Set	Specimen Code	Ultimate Load P_u (kN)	Max. Strain (μ£)	Lateral Displacement (mm)	Failure Mode
S1	C	141.68	562.675	----	Local failure at the column ends
	S	154.56	1247.84	0.976	Steel local buckling
S2	PC-C	175.17	1930	---	
	R25G-C	149.41	1803	---	Concrete crushing
	R25C-C	141.86	1687	----	
	R50G-C	131.37	1597	---	
S3	CPC-C	654.3	1802.85	10.08	
	CR25G-C	575.73	14163.5	9.109	Global buckling
	CR25C-C	552.55	4003.795	4.773	
	CR50G-C	547.4	14413.2	4.334	
S4	CPC-S	604.07	2937.77	---	
	CR25G-S	537.09	3754.03	----	Steel local buckling
	CR25C-S	533.233	1612.42	-----	
	CR50G-S	504.89	1461.71	23.52	Global buckling

Table 9. Experimental and numerical of concrete filled circular steel tubular columns.

Specimen Code	$P_{Exp.}$ (kN)	FE		AISC-LRFD (1999)		AISC-LRFD (2005)		EC4 (1994)	
		P_{FE} (kN)	P_{Exp} / P_{FE}	P_U (kN)	P_u / P_{Exp}	P_U (kN)	P_u / P_{Exp}	P_U (kN)	P_u / P_{Exp}
CPC-C	654.3	595.4	1.098	590.8	0.903	602.6	0.921	635.98	0.972
CR25G-C	575.73	526.7	1.092	521.5	0.906	548.6	0.953	622.90	1.082
CR25C-C	533.233	513.8	1.075	482.8	0.88	507.5	0.925	570.64	1.04
CR50G-C	504.89	488.3	1.121	487.8	0.883	508.8	0.921	540.34	0.978
Mean	-	-	1.097	-	0.893	-	0.93	-	1.018

Table 10. Experimental and numerical ultimate loads of concrete filled square steel columns.

Specimen Code	$P_{Exp.}$ (kN)	FE		AISC-LRFD (1999)		AISC-LRFD (2005)		EC4 (1994)	
		P_{FE} (kN)	P_{Exp} / P_{FE}	P_U (kN)	P_u / P_{Exp}	P_U (kN)	P_u / P_{Exp}	P_U (kN)	P_u / P_{Exp}
CPC-S	604.7	575.1	1.053	561.2	0.927	553.9	0.915	619.8	1.024
CR25G-S	537.09	474.5	1.064	464.5	0.92	458.4	0.908	511.96	1.014
CR25C-S	534.54	475.7	1.123	500.9	0.937	494.4	0.925	552.7	1.034
CR50G-G	537.09	494.1	1.086	491.4	0.915	484.9	0.903	541.3	1.008
Mean	-	-	1.081	-	0.924	-	0.912	-	1.020

Fig. 11. Failure mode of tested specimens.
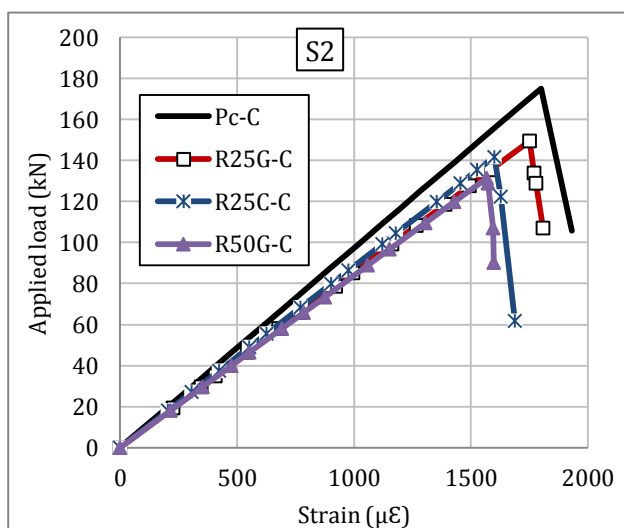

Fig. 12. Applied load-strain curve for S2 specimens.
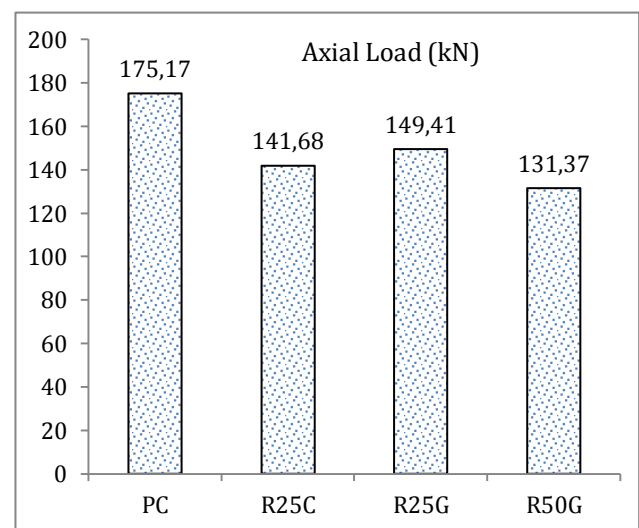

Fig. 13. Comparison between tested specimens of S2.
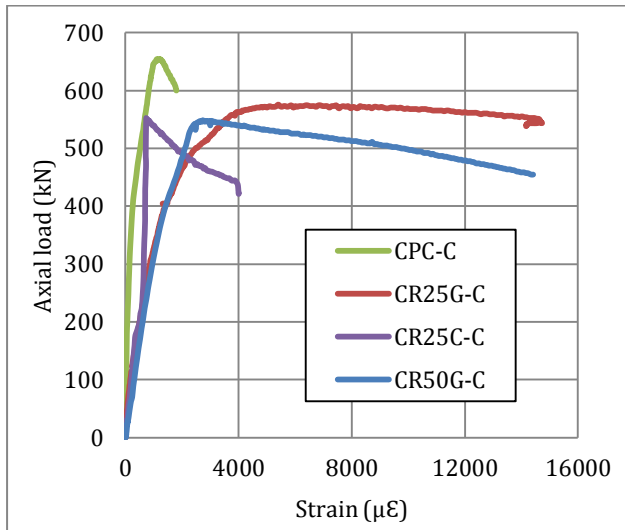
Fig. 14. Applied load-strain curve for S3 specimens.
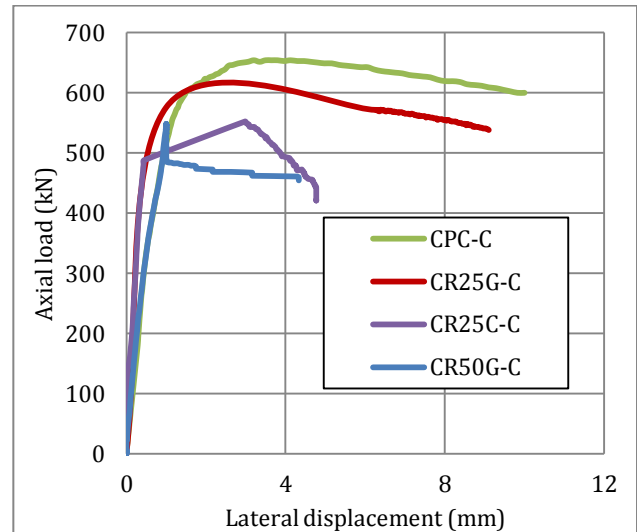

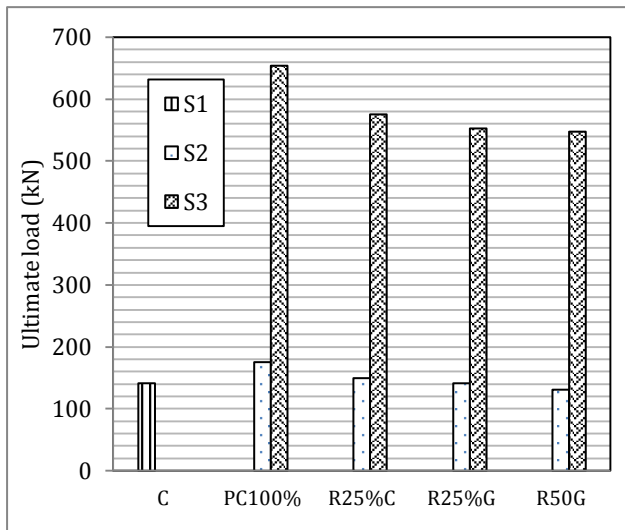**Fig. 15.** Applied load-lateral displacement curve for S3 specimens.
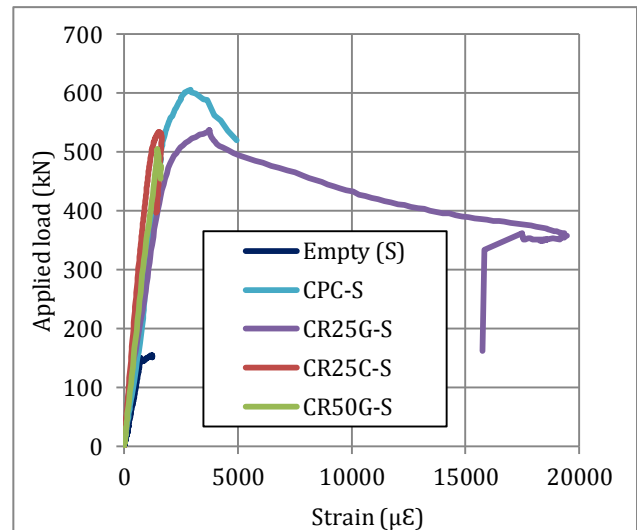

Fig. 16. Ultimate load for all circular specimens.

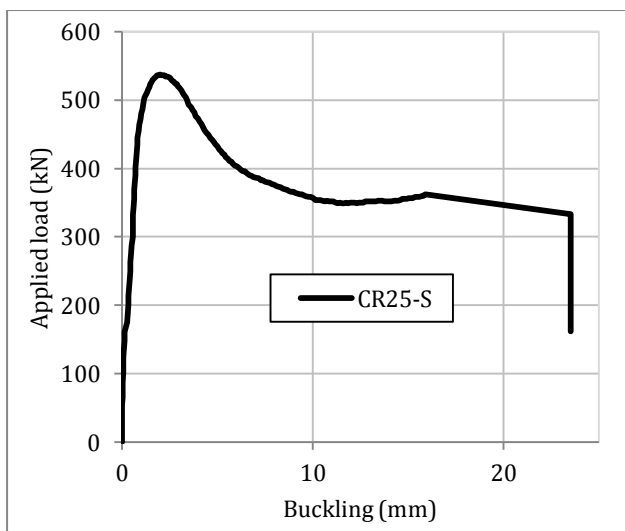**Fig. 17.** Applied load-strain curve for S4 specimens.

Fig. 18. Load-buckling curve of CR25-S specimens.
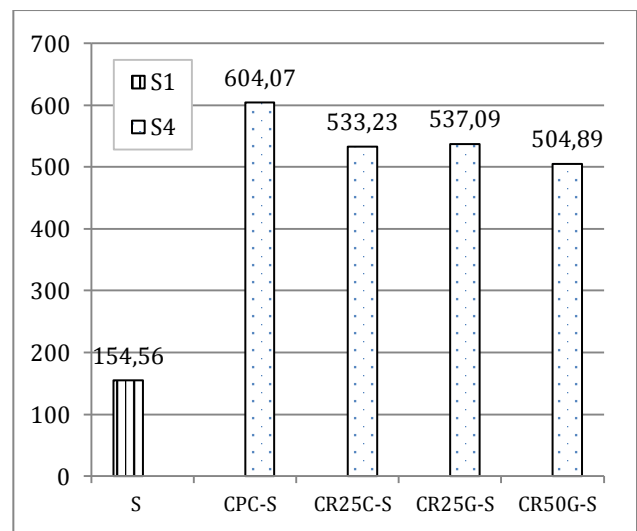

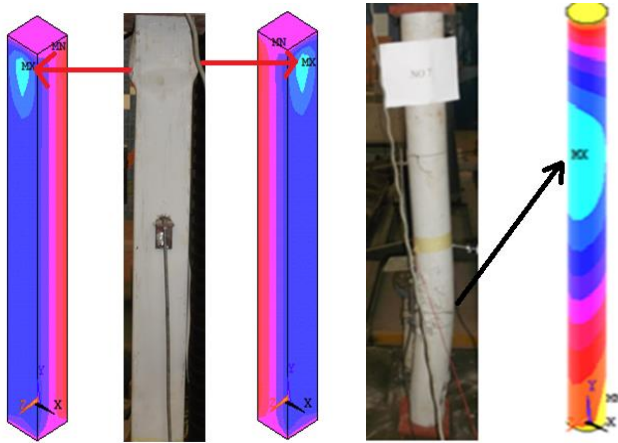**Fig. 19.** Ultimate load of box column.

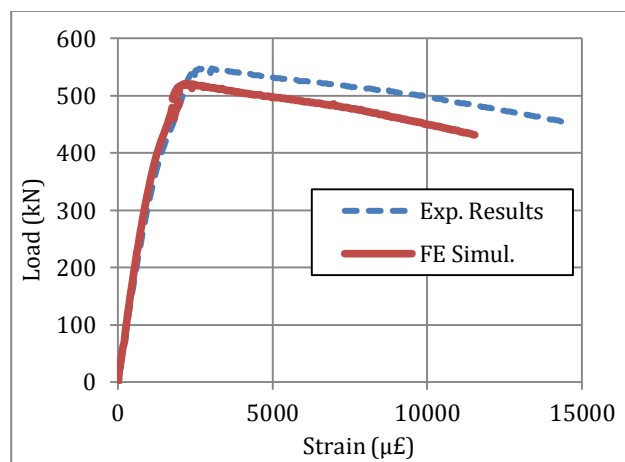**Fig. 20.** Experimental and FE simulation failure modes.

Fig. 21. Experimental and numerical load-axial strain for specimen CR50G-C as a sample.

5. Conclusions

The main objective of this study is to evaluate the structural behavior of recycled aggregates concrete-filled steel tubular columns under compression forces up to failure as well as to examine the effects of different parameters that recycled aggregates ratio, type of recycled aggregates, steel tube shape and the effect of the composite action. The study consisted of an experimental investigation, theoretical and numerical study. A total of fourteen specimens were cast and tested under compression axial loading conditions in the laboratories of the Housing and Building National Research Center, Egypt. The modes of failure, the ultimate capacities and the general deformational behavior of the specimens, based on the measured strain and buckling introduced and the cracking behavior of specimens were presented and discussed. Analytical models by finite element method were employed for the composite specimens and were compared with the experimental results. The composite specimens were also analyzed by different national building codes such as AISC-LRFD (1999), AISC-LRFD (2005) and European code EC4 (2004). Also the experimental, analytical and numerical results were compared. Based on the results of this study, the following conclusions can be drawn:

- The typical failure modes of Recycled Aggregates Concrete Filled Steel Tube (RACFST) columns are similar to those of the normal CFST columns. They were all failed due to buckling.
- The ultimate capacities of composite columns successfully increased more than 250 percent compared with concrete or steel columns.
- The recycled aggregates concrete filled columns have slightly lower but comparable ultimate capacities compared with the filled specimens with normal concrete. The ultimate capacities of the filled steel circular column with normal concrete were about 8 and 16 percent higher than those containing 25 and 50 percent recycled coarse aggregates; respectively.
- For square filled steel tube column with normal concrete, the increasing ranges are about 11 and 17 percent. The lowering in capacities of RACFST columns can be attributed to the lower strength of recycled aggregates concrete as compared to normal concrete.
- The ultimate load of columns with circular section is greater than ultimate load of columns with square section by about 30 to 40 percent. This is because circular section takes confining effect better than square section.
- It was found that, the FE model gives good results comparing with the experimental results.
- From the results of this study, it is proved that RAC has given acceptable results comparing with NPC. Moreover using RAC preserves the environment and reduces the cost of construction.
- AISC-LRFD (1999) and AISC-LRFD (2005) gives ultimate capacity about 11 and 7 percent respectively; lower than the ultimate capacity obtained from the tests.
- EC4 (2004) gives a member capacity about 1.0 to 3.4 percent higher than the experimental result for circular and square RACFST columns respectively.
- Composite specimens have given ductility failure behavior comparing with concrete and steel specimens. This leads to an early warning before complete failure occurring.

References

Aboul-Anen B, El-Shafey A, El-Shami M (2009). Experimental and analytical model of ferrocement slabs. *International Journal of Recent Trends in Engineering*, 1(6), 25-29.

AISC-LRFD (1999). Load and resistance factor design specification for structural steel buildings. American Institute of Steel Construction, Chicago, USA.

AISC-LRFD (2005). Specification for structural steel buildings. American Institute of Steel Construction, Chicago, USA.

ANSYS (2006). Help and Manual. ANSYS Inc., PA, USA.

Bradford MA, Loh HY, Uy B (2002). Slenderness limits for filled circular steel tubes. *Journal of Constructional Steel Research*, 58, 243-252.

Butler L, West JS, Tighe SL (2011). The effect of recycled concrete aggregate properties on the bond strength between RCA concrete and steel reinforcement. *Cement and Concrete Research*, 41, 1037-1049.

Campian C, Nagy Z, Pop M (2015). Behavior of fully encased steel-concrete composite columns subjected to monotonic and cyclic loading. *Procedia Engineering*, 117, 439-451.

Chen J, Jin WL (2010). Experimental investigation of thin-walled complex section concrete-filled steel stub columns. *Journal of Thin-Walled Structures*, 48, 718-724.

E.C.P. 203/2007 (2007). Egyptian code of practice: design and construction for reinforced concrete structures. Research Centre for Houses Building and Physical Planning, Cairo, Egypt.

E.S.S. 1109/2008 (2008). Egyptian standard specification for aggregates. Egyptian Standard Specification. Ministry of Industry, Cairo, Egypt.

E.S.S. 2070/2007 (2007). Egyptian standard specifications for plain and reinforcement concrete. Egyptian Standard Specification. Ministry of Industry, Cairo, Egypt.

E.S.S. 4756-1/2009 (2009). Egyptian standard specification for ordinary Portland cement. Egyptian Standard Specification. Ministry of Industry, Cairo, Egypt.

Etxeberria M, Vázquez E, Marí A, Barra M (2007). Influence of amount of recycled coarse aggregates and production process on properties of recycled aggregate concrete. *Cement and Concrete Research*, 37, 735-742.

Eurocode 4 (2004). European standard: design of composite steel and concrete structures. European Committee for Standardization, Brussels, Belgium.

Evangelista L, de Brito J (2007). Mechanical behavior of concrete made with fine recycled concrete aggregates. *Cement & Concrete Composites*, 29, 397-401.

Gomez-Soberon JMV (2002). Porosity of recycled concrete with substitution of recycled concrete aggregate; an experimental study. *Cement and Concrete Research*, 32, 1301-1311.

Hoque M (2006). 3D Nonlinear Mixed Finite-Element Analysis of RC Beams and Plates with and without FRP Reinforcement. *M.Sc. thesis*. University of Manitoba, Winnipeg, Manitoba, Canada.

Lam D, Gardner L (2008). Structural design of stainless steel concrete filled columns. *Journal of Constructional Steel Research*, 64, 1275-1282.

Liang QQ (2012). Biaxial loaded high-strength concrete-filled steel tubular slender beam-columns, Part I: Multiscale simulation. *Journal of Constructional Steel Research*, 75, 64-71.

Mander JB, Priestley MJN, Park R (1988). Theoretical stress-strain model for confined concrete. *Journal of Structural Engineering, ASCE*, 114(8), 1804-1826.

Marco Breccolotti M, Materazzi AL (2010). Structural reliability of eccentrically-loaded sections in RC columns made of recycled aggregate concrete. *Engineering Structures*, 32, 3704-3712.

Oikonomou ND (2005). Recycled concrete aggregates. *Cement & Concrete Composites*, 27, 315-318.

Patel V, Lande PS (2016). Analytical behavior of concrete filled steel tubular columns under axial compression. *International Journal of Engineering Research*, 5(Special 3), 629-632.

Patton ML, Singh KD (2014). Finite element modeling of concrete-filled lean duplex stainless steel tubular stub columns. *International Journal of Steel Structures*, 14(3), 619-632.

Poon CS, Shui ZH, Lam L, Fok H, Kou SC (2004). Influence of moisture states of natural and recycled aggregates on the slump and compressive strength of concrete. *Cement and Concrete Research*, 34, 31-36.

Sakino K, Nakahara H, Morino S, Nishiyama I (2004). Behavior of centrally loaded concrete- filled steel-tube short columns. *Journal of Structural Engineering*, 2(130), 180-8.

Salem AH (1970). Extension of stability considerations to the simple plastic theory. *The Bulletin of the Faculty of Engineering,* No. 4, Ain Shams University, Egypt.

Schneider SP (1998). Axially loaded concrete-filled steel tubes. *Journal of Structural Engineering*, 10(124), 1125-38.

Schubert S, Hoffmann C, Leemann A, Moser K, Motavalli M (2012). Recycled aggregate concrete: experimental shear resistance of slabs without shear reinforcement. *Engineering Structures*, 41, 490-497.

Shaheen YBI, Eltaly B, Abdul-Fataha S (2014). Structural performance of ferrocement beams reinforced with composite materials. *Structural Engineering and Mechanics*, 50(6), 817-834.

Shaheen YBI, Eltaly B, Kameel M (2013). Experimental and analytical investigation of ferrocement water pipe. *Journal of Civil Engineering and Construction Technology*, 4(4), 157-167.

Shanmugam NE, Lakshmi B (). State of art report on steel-concrete composite columns. *Journal of Constructional Steel Research*, 57, 1041-80, 2001.

Singh G (2006). Finite Element Analysis of Reinforced Concrete Shear Walls. *M.Sc. thesis*. Deemed University, India.

Uy B (1998). Local and post-local buckling of concrete filled steel welded box columns. *Journal of Constructional Steel Research*, 47, 47-72.

Uy B (2001). Strength of short concrete filled high strength steel box columns. *Journal of Constructional Steel Research*, 57, 113-134.

Vazirani VN, Ratwani MM (1996). Analysis of Structures. Textbook for Engineering Students, Khanna Publishers, China.

Wilson EL, Taylor RL, Doherty WP, Ghaboussi J (1973). Incompatible Displacement Models. *In: Numerical and Computer Methods in Structural Mechanics*. Academic Press, Inc., New York and London, 43-57.

Zega CJ, Di Maio AA (2011). Use of recycled fine aggregate in concretes with durable requirements. *Waste Management*, 31(11), 2336-2340.

Zuboski GR (2013). Stress-strain behavior for actively confined concrete using Shape Memory Alloy Wires. *Ph.D thesis*. The Ohio State University, Columbus, USA.